JOURNAL OF VIROLOGY, Feb. 2003, p. 1747–1756 Vol. 77, No. 3
0022-538X/03/$08.00+0 DOI: 10.1128/JVI.77.3.1747–1756.2003

Role of Plasma Membrane Lipid Microdomains in Respiratory Syncytial Virus Filament Formation

Lewis H. McCurdy and Barney S. Graham*

Vaccine Research Center, National Institute of Allergy and Infectious Diseases, National Institutes of Health, Bethesda, Maryland

Received 10 May 2002/Accepted 28 October 2002

The fusion protein (F) of respiratory syncytial virus (RSV) is the envelope glycoprotein responsible for the characteristic cytopathology of syncytium formation. RSV has been shown to bud from selective areas of the plasma membrane as pleomorphic virions, including both filamentous and round particles. With immunofluorescent microscopy, we demonstrated evidence of RSV filaments incorporating the fusion protein F and colocalizing with a lipid microdomain-specific fluorescent dye, 1,1-dihexadecyl-3,3,3,3-tetramethylindocarbocyanine perchlorate. Western blot analysis of Triton X-100 cold-extracted membrane fractions confirmed the presence of RSV proteins within the lipid microdomains. RSV proteins also colocalized with cellular proteins associated with lipid microdomains, caveolin-1, and CD44, as well as with RhoA, a small GTPase. ADP-ribosylation of RhoA by *Clostridium botulinum* exotoxin inactivated RhoA signaling and resulted in the absence of RSV-induced syncytia despite no significant change in viral titer. We demonstrated an overall decrease in both the number and length of the viral filaments and a shift in the localization of F to nonlipid microdomain regions of the membrane in the presence of C3 toxin. This suggests that the selective incorporation of RSV proteins into lipid microdomains during virus assembly may lead to critical interactions of F with cellular proteins, resulting in microvillus projections necessary for the formation of filamentous virus particles and syncytium formation. Thus, manipulation of membrane lipid microdomains may lead to alterations in the production of viral filaments and RSV pathogenesis and provide a new pharmacologic target for RSV therapy.

Human respiratory syncytial virus (RSV) belongs to the *Pneumovirus* genus of the *Paramyxoviridae* family and is the leading cause of viral respiratory illness in children, accounting for over 100,000 hospitalizations in the United States yearly (37). More recently, RSV has been recognized as a significant pathogen among the elderly (15), nursing home patients (8), and bone marrow and lung transplant recipients (16, 30, 42). In bone marrow transplant recipients infected with RSV, the pathology involves extensive syncytium formation, described as giant-cell pneumonia, for which mortality rates approach 80% (16). Given the significant morbidity and mortality, the development of new antiviral agents for both RSV prophylaxis and therapy is an area of clinical importance and active research.

The RSV virion consists of a lipid envelope that incorporates three transmembrane glycoproteins, F, G, and SH. The G protein is thought to be involved in viral attachment (20), possibly via its binding to cellular sulfated heparin-like glycosaminoglycans (10, 19). The fusion protein F is essential for both virus-to-cell fusion and cell-to-cell fusion, demonstrated by inhibition of syncytium formation with monoclonal antibodies against F (41). Recombinant viruses expressing only the RSV F protein and a mutant RSV virus, cp-52, lacking the G and SH genes are capable of forming syncytia, which provides further evidence for the important role of F in virus entry and RSV pathogenesis (17, 40).

The F protein has been shown to interact with RhoA, a small GTPase binding protein in the Ras superfamily (31). RhoA is ubiquitous in mammalian cells and is involved in a variety of cellular functions, including gene transcription, cell cycle progression, cell morphology, and actin reorganization (18, 25). RhoA requires activation that involves the exchange of GDP for GTP, followed by geranylgeranylation at the carboxy terminus before translocation to the inner leaflet of the plasma membrane (1). Inhibitors of RhoA isoprenylation, including 3-hydroxy-3-methylglutaryl coenzyme A (HMG-CoA) reductase inhibitors, have been demonstrated to decrease RSV infection in vitro and in vivo (12).

RhoA activation initiates multiple signaling pathways, leading to effects on cell function and structure, including the formation of actin stress fibers and focal adhesions (33). In vitro, RSV infection activates RhoA and increases membrane-bound RhoA, resulting in an increase in stress fiber formation (11). In addition, RSV-induced syncytium formation has been shown to be dependent on RhoA signaling activity, and viral filament formation appears to be required for syncytium formation (32; T. L. Gower, M. K. Pastey, M. Peebles, P. Collins, T. K. Hart, A. Guth, and B. S. Graham, submitted for publication).

The F protein has been demonstrated to interact with RhoA in vitro. RSV-induced syncytium formation is inhibited by a RhoA-derived peptide, and treatment with the RhoA-derived peptide inhibits RSV infection in an in vivo mouse model (32). While this suggests a critical interaction between the F protein and RhoA in RSV pathogenesis, the exact events involved are not known.

Lipid microdomains, or lipid rafts, are highly liquid-ordered areas of the plasma membrane that are rich in cholesterol and sphingolipids and are insoluble in nonionic detergents such as Triton X-100 at low temperatures (38). Recent studies suggest

* Corresponding author. Mailing address: Vaccine Research Center, NIAID, National Institutes of Health, Building 40, Room 2502, 40 Convent Dr., MSC 3017, Bethesda, MD 20892-3017. Phone: (301) 594-8468. Fax: (301) 480-2771. E-mail: bgraham@nih.gov.

that cell sorting and cellular signaling may occur selectively through these areas (4). Lipid microdomains are enriched in glycosylphosphatidylinositol-anchored proteins and acylated proteins, including the transmembrane influenza virus hemagglutinin (HA) protein and caveolin-1. The association of the HA protein with lipid microdomains has led to the understanding of the preferred budding of influenza virus from lipid rafts (36, 45).

Other viruses have subsequently been shown to selectively bud from lipid microdomains, including another member of the *Paramyxoviridae* family, measles virus, Ebola virus, and human immunodeficiency virus (HIV) (3, 24, 26). Through manipulation of the cholesterol content of the plasma membrane, HIV virus production and syncytium formation can be reduced (21, 23, 28). Since RSV F has properties similar to those of the fusion protein of HIV, gp41, we hypothesized that RSV assembly and budding also occur in lipid rafts and that F may potentially interact with membrane-bound RhoA within these specialized areas of the host cell.

In this study, we sought to identify the cellular association of RSV proteins and host proteins within the lipid microdomain. By using sucrose gradient centrifugation and immunofluorescent microscopy, colocalization of the F protein and RhoA was shown to occur within the lipid raft fraction of the plasma membrane. In addition, CD44 transmembrane protein colocalized with F and RhoA. These interactions may be paramount to viral filament formation, which is necessary for RSV-induced syncytium formation.

MATERIALS AND METHODS

Virus and cells. The A2 strain of RSV was originally provided by R. Chanock, National Institutes of Health, Bethesda, Md. RSV stocks were prepared as previously described (13). HEp-2 cells were maintained in Eagle's minimal essential medium supplemented with glutamine, gentamicin, penicillin G, and 10% fetal bovine serum.

Antibodies, dyes, and reagents. Primary antibodies used for immunofluorescence to detect RSV included a rabbit polyclonal antibody to RSV proteins and a mouse monoclonal antibody for the RSV F protein, gifts of James Crowe, Vanderbilt University, Nashville, Tenn. Western blot analysis for RSV proteins was performed with a horseradish peroxidase-conjugated goat polyclonal antibody from Fitzgerald Industries (Concord, Mass.). Primary mouse monoclonal antibody for RSV N protein was purchased from Accurate Chemical (Westbury, N.Y.), CD44 antibody was from Sigma Pharmaceuticals (St. Louis, Mo.), transferrin receptor antibody was from Zymed Labratories (San Francisco, Calif.), and RhoA antibody was from Santa Cruz Biotechnologies (Santa Cruz, Calif.). Caveolin-1 rabbit polyclonal antibody was obtained from BD Transduction (Franklin Lakes, N.J.), and CD44 rabbit polyclonal antibody was from Santa Cruz Biotechnologies. Secondary antibodies included fluorescein isothiocyanate (FITC)-labeled goat anti-rabbit immunoglobulin and anti-mouse immunoglobulin antibodies and rhodamine-labeled goat anti-rabbit immunoglobulin and anti-mouse immunoglobulin antibodies (Molecular Probes, Eugene, Oreg.). Dialkylcarbocyanine dyes $DiIC_{12}(3)$ (1,1-didodecyl-3,3,3,3-tetramethylindocarbocyanine perchlorate) and $DiIC_{16}(3)$ (1,1-dihexadecyl-3,3,3,3-tetramethylindocarbocyanine perchlorate), used for selective labeling of lipid membranes, were obtained from Molecular Probes (Eugene, Oreg.). *Clostridium botulinum* exotoxin (C3 toxin) was obtained from Calbiochem (La Jolla, Calif.).

Immunofluorescence assay. HEp-2 cells were plated on coverslips in six-well plates and infected with RSV (100 μl of a 4×10^5 PFU/ml stock). Following a 24-h incubation period post-RSV infection, cells were prepared for analysis by immunofluorescent microscopy. Cells were fixed with 3.7% formaldehyde for 10 min, followed by 0.5% Triton X-100 for 10 min, and then incubated with 5% dry milk–phosphate-buffered saline (PBS) for 15 min to reduce nonspecific binding. Fixed cells were then incubated with primary antibodies in 3% dry milk–PBS at a 1:50 to 1:100 dilution for 1 h and washed with PBS three times. Secondary antibodies diluted at 1:200 in 3% dry milk–PBS were added, and cells were incubated for 1 h- followed by washing with PBS three times. After fixing the slides, viewing was performed with Zeiss Axiovert and Axioplan light microscopes at 40× and 100× oil immersion. Fluorescent images were obtained with a Zeiss AttoArc2 lamp and filter sets 41001 and 41002b from Chroma Technology Corporation (Brattleboro, Vt.). Images were obtained and analysis was performed with Adobe Photoshop software; brightness and contrast were adjusted for viewing.

Immunofluorescence with lipid dye analogs. HEp-2 cells were infected with RSV as described above for 24 h. Six-well plates were then placed on ice and washed with cold PBS, and then 500 μl of $DiIC_{12}(3)$ and $DiIC_{16}(3)$ at a 1:100 dilution in ethanol were added to each well for 15 min. Cells were then washed with PBS and fixed with 3.7% formaldehyde as above. Primary and secondary antibodies were then used as indicated.

Detergent extraction and flotation centrifugation. HEp-2 cells were infected with RSV at a multiplicity of infection of 1.0 for 1 h at room temperature. Cells were then incubated at 37°C for 24 h and washed with PBS. Prior to sucrose gradient flotation, select monolayers were treated with 10 mM methyl-β-cyclodextrin (Sigma Chemical, St. Louis, Mo.) for 30 min at 37°C. Sucrose gradient flotation was performed as previously described with minor modification (5). Cells were lysed in 2 ml of TNE buffer (50 mM Tris-HCl, 150 mM NaCl, 5 mM EDTA) containing 1% Triton X-100 and protease inhibitors (Roche Diagnostics, Mannheim, Germany) at 4°C for 30 min, followed by centrifugation at 2,000 rpm for 10 min. The postnuclear supernatant was removed, loaded into SW41 tubes, mixed with 2 ml of 80% sucrose, and layered with 5.0 ml of 35% and 3.0 ml of 5% sucrose. The gradient underwent centrifugation at 4°C for 16 h at 35,000 rpm in a Beckman SW41 rotor. Twelve 1-ml fractions were harvested from the top to the bottom of the gradient.

Protein precipitation, analysis, and blotting. Samples were subjected to methanol precipitation according to the protocol of Wessel and Flugge (43). Two-hundred-microliter aliquots were precipitated by adding 0.8 ml of methanol, followed by 0.2 ml of chloroform. After centrifugation, distilled water was then added at 0.6 ml for phase separation, and the sample was vortexed and then centrifuged for 1 min at 13,000 rpm. The upper phase was removed and discarded. Methanol was added at 0.6 ml, and then the protein pellet was obtained by centrifugation at 13,000 rpm for 2 min. Protein was suspended in 5% sodium dodecyl sulfate and quantified with the BCA assay (Pierce, Rockford, Ill.). Equal amounts of protein from aliquots 3 to 11 were analyzed by sodium dodecyl sulfate-polyacrylamide gel electrophoresis (PAGE) and Western blotting. Densitometry was performed with a GS-800 scanner and Quantity One software from Bio-Rad Laboratories (Hercules, Calif.).

Treatment with C3 toxin. HEp-2 cells were grown on coverslips in 24-well plates. Cells were treated with 250 μl of C3 toxin at 30 μg/ml and incubated overnight at 37°C. Medium was removed, and cells were infected with 100 μl of RSV at 4×10^5 PFU/ml. After 1 h at room temperature, 250 μl of C3 toxin-containing medium was replaced, and cells were allowed to incubate at 37°C overnight. At 24 h postinfection, cells were evaluated by immunofluorescent staining as described above.

RESULTS

RSV produces viral filaments that involve the F protein and the lipid microdomain. Previous studies have demonstrated the presence of both filamentous and round particles budding from the surface of RSV-infected cells (9, 34). The filamentous particles resemble microvilli in their diameter (80 to 120 nm) but are longer, varying in length from 4 to 8 μm. Filamentous projections can be seen originating from the cell surface of cells infected with RSV (Fig. 1). The role of viral filaments in RSV infection remains uncertain. However, the use of selective filtration of viral particles suggests that the long filaments may be the more infectious form of RSV (34).

With F-specific antibody, we were able to demonstrate the presence of the F protein on viral filaments by immunofluorescent microscopy. HEp-2 cells were infected with RSV at a multiplicity of infection of 1.0 and, 24 h after infection, stained with monoclonal antibody to the F protein (Fig. 2A). The fusion protein was demonstrated on the filamentous projections associated with RSV-infected cells as well as on budding round virions, suggesting a wide distribution of the F protein.

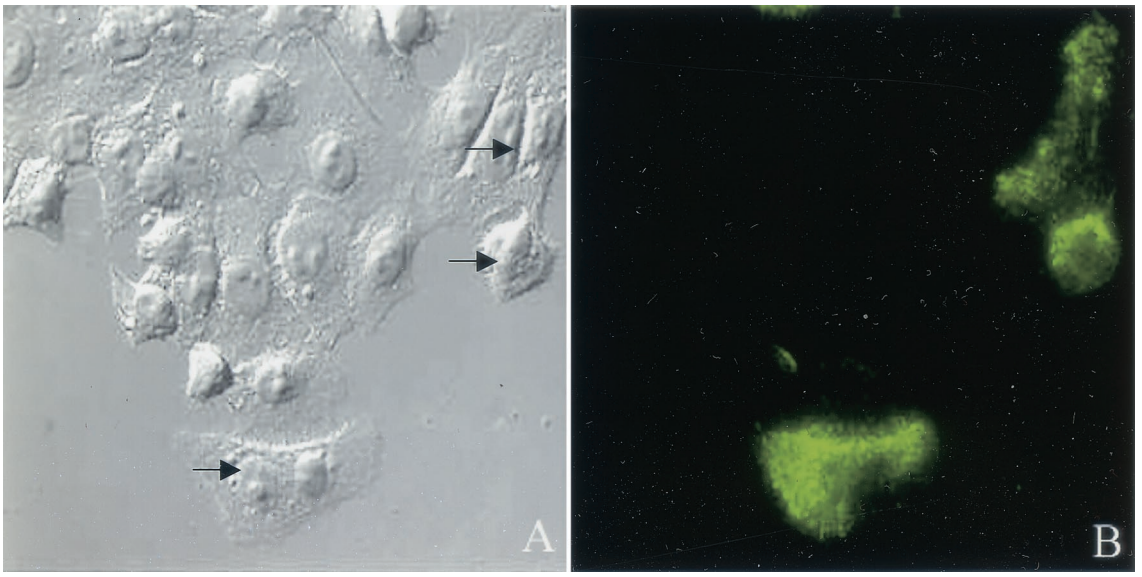

FIG. 1. RSV-infected HEp-2 cells demonstrate morphological changes characterized by filaments which label with anti-RSV antibody. HEp-2 cells were infected with RSV at a multiplicity of infection of 1.0 and incubated at 37°C for 24 h. Cells were fixed with 3.7% formaldehyde and blocked with 5% dry milk–PBS. Cells were incubated with rabbit polyclonal anti-RSV antibody followed by FITC-labeled goat anti-rabbit IgG antibody. RSV-infected cells are distinguished by their FITC labeling with fluorescent microcopy (green). The morphology of noninfected and infected (indicated by arrows) was compared by Nomarski differential interference contrast with a 40× objective.

This confirms our findings with electron microscopy, which demonstrate the presence of F on the surface of viral filaments (Gower et al., submitted).

With a monoclonal antibody to the N protein of RSV, we were also able to show the presence of the N protein associated with filamentous structures projecting from the membrane surface (Fig. 2B). The N protein is part of the nucleocapsid, and its identification within the filaments further supports the idea that the filaments represent viral particles budding from the cell surface. $DiIC_{16}(3)$ and $DiIC_{12}(3)$ are long-chain dialkylcarbocyanine fluorescent lipid dyes which partition preferentially into different domains of the plasma membrane. $DiIC_{16}(3)$ has been shown to incorporate in liquid-ordered domains, while $DiIC_{12}(3)$ is incorporated in fluid domains (39). Images of RSV-infected HEp-2 cells stained with $DiIC_{16}(3)$ demonstrated the presence of viral filaments budding from the cell membrane (Fig. 2C), while there was no evidence of viral filaments in $DiIC_{12}(3)$-stained infected cells (not shown).

RSV proteins RhoA and CD44 are isolated from Triton X-100-insoluble membrane in RSV-infected HEp-2 cells. Identification of proteins associated with the lipid microdomain was performed by cell lysis with the detergent Triton X-100 at 4°C, followed by sucrose gradient centrifugation as previously described (5). Selected fractions were then examined for the

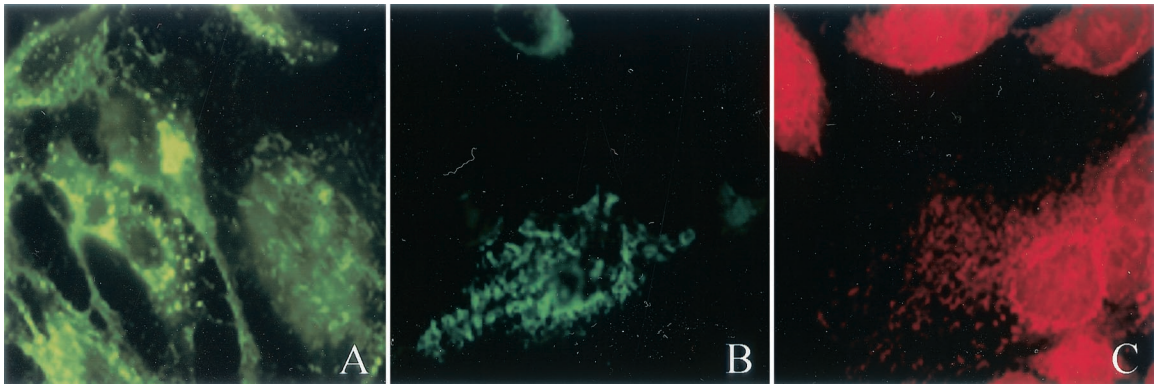

FIG. 2. RSV produces viral filaments which label With both the F and N proteins and with the lipid dye $DiIC_{16}(3)$. HEp-2 cells were infected with RSV at a multiplicity of infection of 1.0 and incubated at 37°C for 24 h. Cells were fixed with 3.7% formaldehyde and permeabilized with 0.5% Triton X. After blocking, cells were incubated with mouse anti-F (A) and anti-N (B) monoclonal antibodies followed by FITC-labeled goat anti-mouse IgG (green). In addition, prior to fixation, RSV-infected HEp-2 cells were incubated on ice with either $DiIC_{12}(3)$ (not shown) or $DiIC_{16}(3)$ (C) for 15 min. Cells were then fixed and imaged in the absence of antibody. Filamentous particles observed budding from the surface of RSV-infected cells demonstrate the presence of both the F and N proteins of RSV and incorporated the lipid dye $DiIC_{16}(3)$, which is specific for the lipid raft.

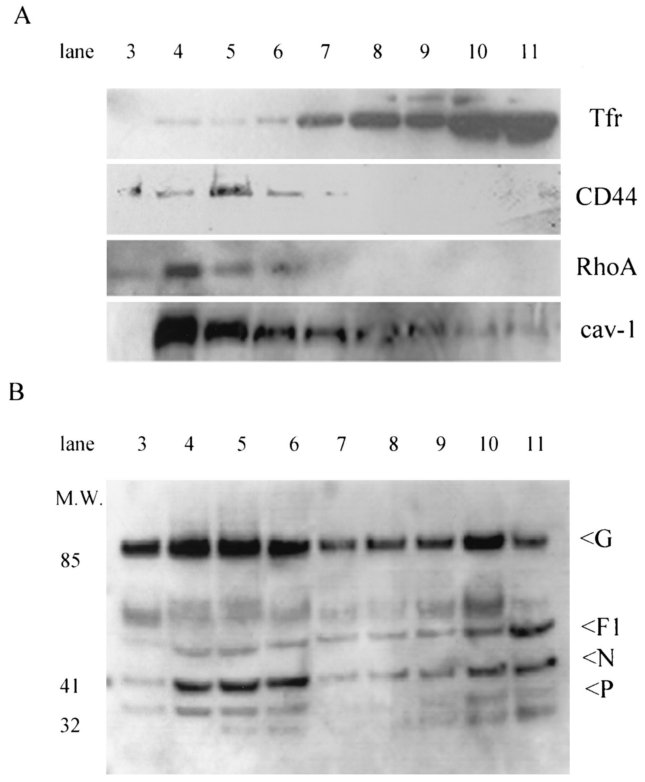

FIG. 3. RSV proteins localize to the detergent-insoluble raft microdomains after sucrose gradient separation. RSV-infected HEp-2 cells were lysed in 1% Triton X-100 at 4°C at 24 h postinfection. Postnuclear extract was layered with a discontinuous sucrose gradient and centrifuged at 35,000 rpm for 16 h, and 1-ml fractions were collected (see Materials and Methods for details). Fraction 1 represents the top of the gradient, 12 represents the bottom, and fractions 3 to 5 are where the cholesterol-rich regions of the membrane localize. Examination of cellular proteins was performed by Western blotting after separation by sodium dodecyl sulfate-PAGE and transfer to polyvinylidene difluoride membranes. (A) CD44 and RhoA localized to fractions 3 to 5 with raft protein caveolin-1 (cav-1), while the nonraft protein transferrin receptor (Tfr) was noted in soluble fractions 8 to 11. (B) Membrane localization of RSV proteins was examined with a goat polyclonal RSV antibody. RSV proteins, including G and F1, are found in both the lipid raft and nonraft fractions, while there is a predominant localization of N and P proteins to the lipid raft domains.

presence of viral and host cellular proteins by Western blot analysis. Immunoblotting of RSV-infected HEp-2 cells demonstrated the presence of both caveolin-1 and CD44 within the Triton X-insoluble fractions (fractions 3 to 5), which corresponds to the raft component of the plasma membrane (Fig. 3A), while the nonraft transferrin receptor was found predominantly within the soluble fractions, 8 to 11 (Fig. 3A). This distribution of caveolin-1 and CD44 within the lipid raft is consistent with previous observations (27).

We then examined the membrane distribution of the GTPase RhoA. Gower et al. have shown that membrane-associated RhoA is increased following RSV infection (11). We showed that 24 h after RSV infection, RhoA migrated with CD44 and was found in detergent-insoluble raft fractions (Fig. 3A). RSV is highly cell associated, and polyclonal antibody directed against RSV demonstrated the presence of viral proteins in both detergent-insoluble and detergent-soluble fractions of the gradient (Fig. 3B). Densitometry performed on Western blots of RSV proteins revealed that a significant fraction of the envelope proteins, F protein (29.9%) and G (61.0%), and the N and P proteins (64.4% and 66.4%, respectively) resided within the lipid microdomain fractions (see Fig. 8B).

Caveolin-1, RhoA, CD44, and F protein colocalize with lipid dye specific for the lipid microdomain. With immunofluorescent markers that selectively partition into liquid-ordered and fluid domains of the plasma membrane, we sought to determine colocalization of viral proteins and cellular proteins with the lipid microdomains. HEp-2 cells were infected with RSV at a multiplicity of infection of 1.0 and, 24 h postinfection, were labeled with either the $DiIC_{16}(3)$ or $DiIC_{12}(3)$ dye for 15 min on ice. After fixation, the cells were labeled with primary antibody, followed by FITC-labeled anti-mouse or anti-rabbit IgG. As predicted by Western blot analysis, caveolin-1, CD44, and RhoA (green) demonstrated principal localization to the lipid microdomain by overlapping with the $DiIC_{16}(3)$ (red), shown by the yellow color (Fig. 4F, L, and R, respectively). In contrast, there was minimal overlap between either caveolin-1, CD44, or RhoA with the nonraft dye $DiIC_{12}(3)$, further supporting the localization of these proteins to the lipid microdomains (Fig. 4C, I, and O, respectively).

Cells were also labeled with a monoclonal antibody against the F protein, followed by FITC-labeled anti-mouse IgG. As previously noted, evidence of filamentous projections containing the F protein was again present (Fig. 5B and E). In addition, RSV-infected cells demonstrated aggregated foci of the F protein, suggesting a selective targeting of virus to the plasma membrane, which has been described previously by Bachi with video microscopy (2). Both the filaments and the aggregated areas of F overlapped the raft dye $DiIC_{16}(3)$, as shown in Fig. 5F. The majority of the labeled F colocalized with the lipid microdomain, while there were some areas in which the fusion protein was excluded from the lipid raft, consistent with Western blot analysis. Although the presence of F protein in the nonraft domain is likely based on Western blot analysis, sections of cells stained with $DiIC_{12}(3)$ demonstrated little evidence of overlap with labeled antibody to the F protein (Fig. 5C).

FIG. 4. Colocalization of caveolin-1, CD44, and RhoA with lipid microdomains in immunofluorescent microscopy. HEp-2 cells were infected with RSV at a multiplicity of infection of 1.0. At 24 h postinfection, cells were incubated with dialkylindocarbocyanine lipid dye $DiIC_{12}(3)$ (panels A, G, and M) or $DiIC_{16}(3)$ (panels D, J, and P) for 15 min on ice (shown in red). Cells were then fixed and labeled with primary antibody, as indicated, followed by FITC-labeled goat anti-mouse IgG (green) Panels B and E represent anti-caveolin-1, H and K represent anti-CD44, and N and Q represent anti-RhoA. Colocalization of the cellular proteins with the respective lipid dye markers is demonstrated in yellow (panels C, F, I, L, O, and R). Consistent with the Western blot analysis, CD44 and RhoA localized to the lipid raft domain along with caveolin-1 in RSV-infected cells.

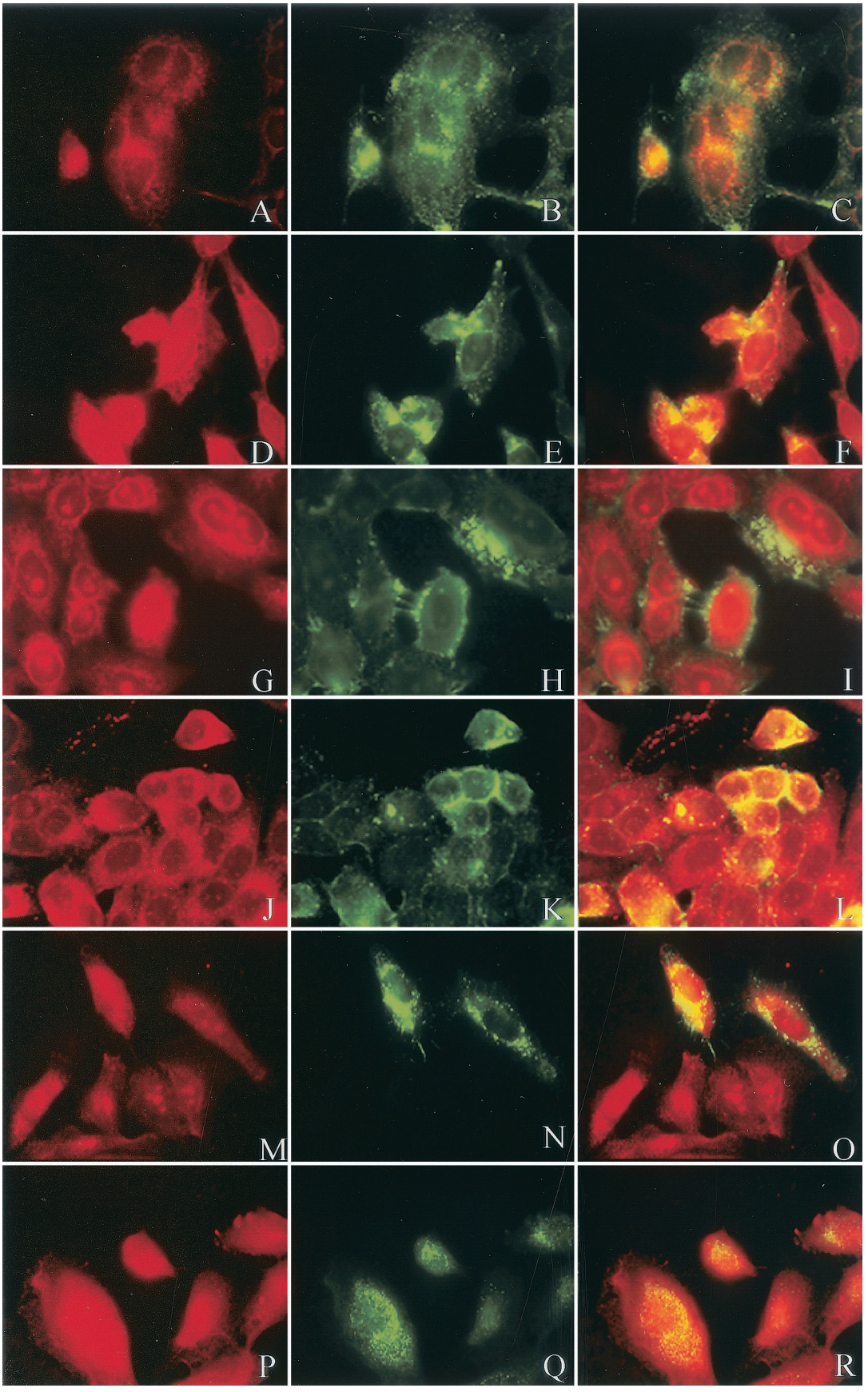
A
B
C
D
E
F
G
H
I
J
K
L
M
N
O
P
Q
R

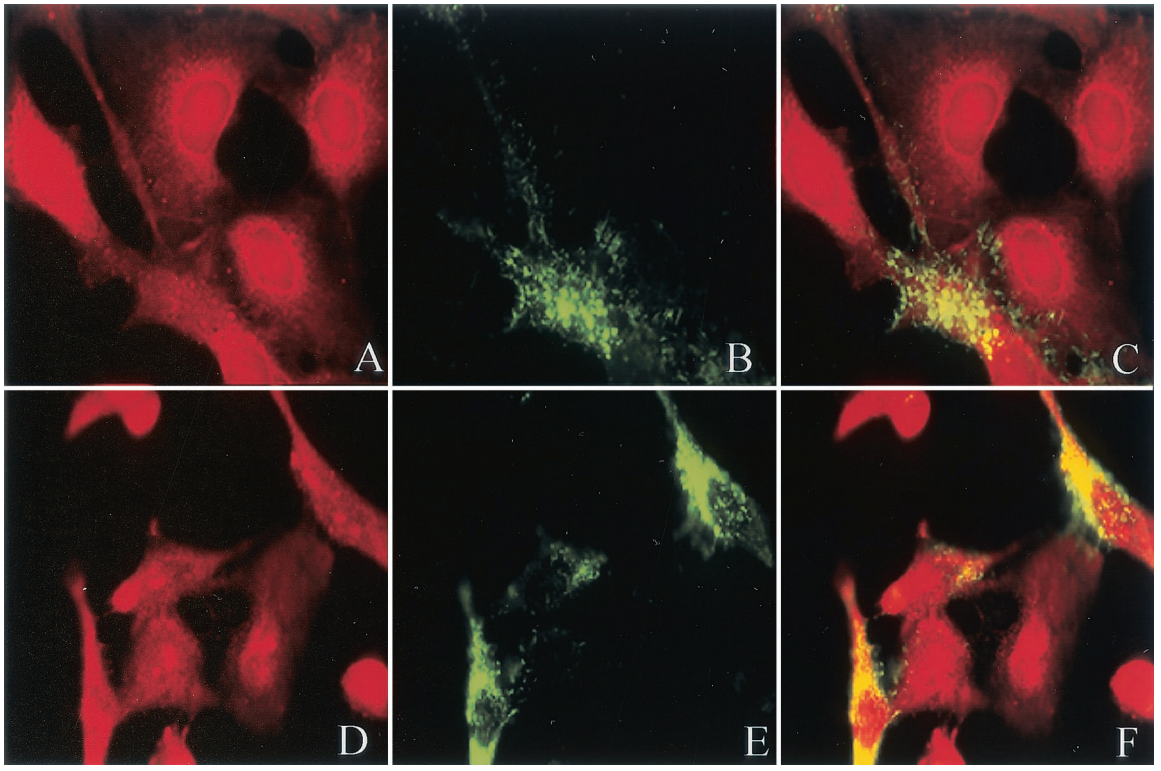

FIG. 5. RSV fusion protein colocalizes with lipid raft dyes $DiIC_{16}(3)$ and not $DiIC_{12}(3)$. At 24 h postinfection, RSV-infected cells were incubated with lipid dye $DiIC_{12}(3)$ (A) or $DiIC_{16}(3)$ (D) for 15 min on ice. Cells were then fixed and labeled with mouse anti-F monoclonal antibody, followed by FITC-labeled anti-mouse IgG, shown in green (B and E). Images demonstrate membrane aggregation of F protein and filament formation. F protein colocalizes preferentially with the lipid dye $DiIC_{16}$ (F) compared to $DiIC_{12}$ (C), as demonstrated in yellow.

RSV proteins overlap caveolin-1, RhoA, and CD44 in infected HEp-2 cells. We used immunofluorescent microscopy to demonstrate colocalization of RSV proteins with RhoA and CD44 (Fig. 6A and D, respectively). RSV proteins labeled with a rabbit polyclonal antibody followed by a secondary FITC-labeled goat anti-rabbit IgG antibody (Fig. 6B) overlapped rhodamine-labeled RhoA (Fig. 6C). With the mouse monoclonal anti-F antibody followed by goat FITC-labeled anti-mouse IgG (Fig. 6E), we also showed overlap with CD44 labeled with a rabbit polyclonal antibody, followed by a rhodamine-labeled goat anti-rabbit IgG (Fig. 6F). This colocalization by immunofluorescent microscopy further supports an interaction of RSV with structural cellular proteins in the lipid microdomains, which was previously demonstrated with caveolin-1 and GM1 (6, 7).

Treatment with C3 toxin alters the morphology of RSV filaments. *Clostridium botulinum* exotoxin (C3 toxin) inhibits effector functions of RhoA. C3 toxin has been shown to block stress fiber formation in RSV-infected HEp-2 cells and to inhibit syncytium formation (11). HEp-2 cells were treated with C3 toxin (30 μg/ml) or left untreated 24 h prior to RSV infection. Cells were then infected with RSV for 1 h and re-treated with C3 toxin or left untreated. Visualization of the cells 24 h postinfection demonstrated a change in the physical characteristics of RSV filaments (Fig. 7B and E). In the presence of C3 toxin, the RSV filaments were both fewer in number and shorter in length. This suggests that while RSV is able to replicate and assemble infectious virions in the absence of RhoA signaling, the assembly and budding of virus are altered.

We next determined the localization of F in C3 toxin-treated cells with the lipid dye analogs $DiIC_{12}(3)$ and $DiIC_{16}(3)$ (Fig. 7A and D). The colocalization of the F protein with the non-lipid dye $DiIC_{12}(3)$ was increased relative to $DiIC_{16}(3)$ in C3-treated RSV-infected cells (Fig. 7C and F) compared to untreated cells (Fig. 5C and F). This suggests the RSV F glycoprotein is not targeted to cholesterol-rich lipid microdomains when RhoA activation is inhibited.

Disruption of lipid microdomains alters the distribution of RSV proteins. Lipid microdomains are characterized by their high content of cholesterol and sphingolipids. Manipulation of the plasma membranes with cyclic oligosaccharides, cyclodextrins, removes cholesterol and disrupts the formation of lipid rafts. After a 24-h infection, we subjected RSV-infected monolayers of HEp-2 cells to 10 mM methyl-β-cyclodextrin for 30 min. Monolayers were then subjected to Triton X-100 at 4°C and layered over a sucrose gradient. Western blot analysis of gradient fractions revealed a nearly complete loss of RSV proteins from the lipid microdomains (Fig. 8A). Densitometry demonstrated a substantial difference in the distribution of RSV proteins compared to that in RSV-infected cells in the absence of cyclodextrin (Fig. 8B). This shows that cholesterol is important to the distribution of viral proteins within the membrane and suggests that manipulation of lipid microdomains may alter the production of infectious virions.

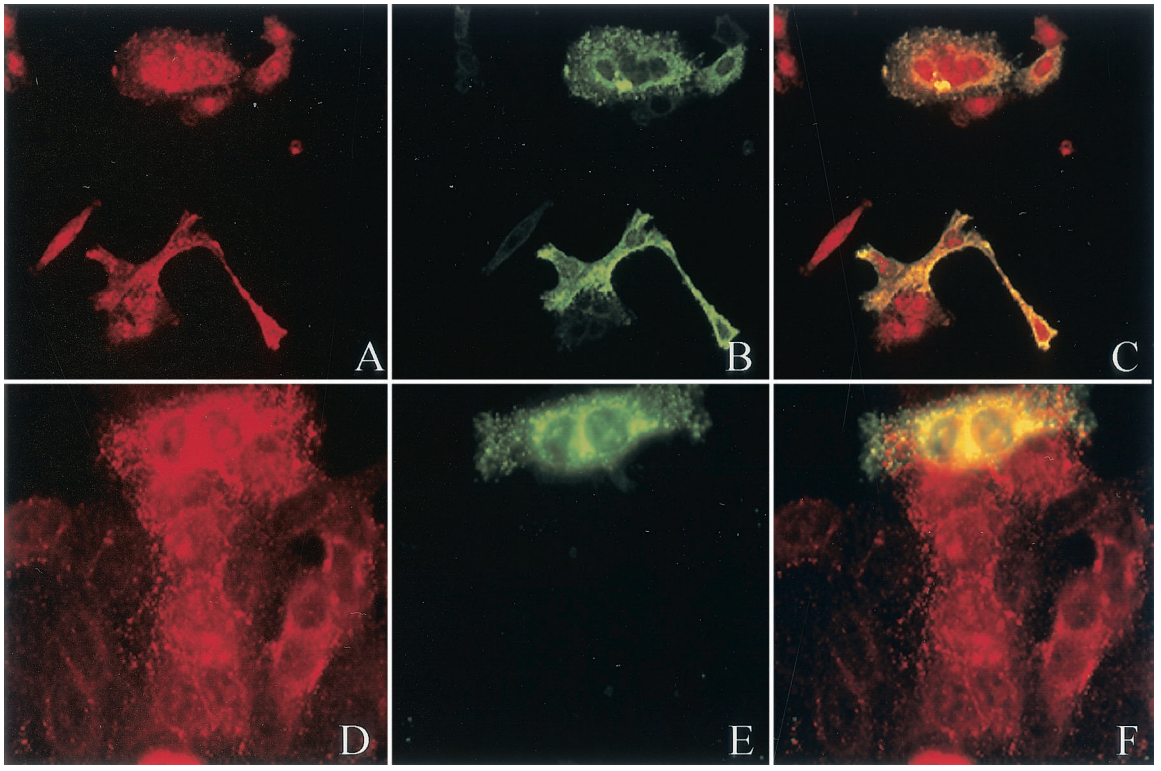

FIG. 6. RSV proteins colocalize with RhoA and CD44. HEp-2 cells were infected with RSV at a multiplicity of infection of 1.0, and 24 h postinfection they were fixed and stained with the primary antibody, mouse monoclonal anti-RhoA (A) or rabbit polyclonal anti-CD44 (D). Simultaneously, cells were stained with either rabbit polyclonal anti-RSV (B) or mouse monoclonal anti-F (E) antibody. Cells were then stained with rhodamine-labeled goat anti-mouse or anti-rabbit IgG (red) and FITC-labeled goat anti-mouse or anti-rabbit IgG (green). The overlap between anti-RhoA and anti-RSV is shown in panel C (yellow) and the overlap between anti-CD44 and anti-RSV is shown in panel F (yellow). Antibodies against both CD44 and RhoA demonstrate overlap with RSV proteins, suggesting colocalization of the cellular proteins with RSV in infected cells.

DISCUSSION

RSV accounts for significant morbidity among infants and selected immunocompromised hosts. Similar to other paramyxoviruses, it is a lipid-enveloped virus which consists of a fusion protein, F, incorporated into the viral membrane, in addition to its other envelope proteins, G and SH. The F protein of RSV is essential for the characteristic cytopathology of RSV, marked by the formation of syncytia. In vitro evaluation of RSV has revealed the presence of pleomorphic viral particles emanating from infected cells, including both round and long filamentous structures. The latter resemble cellular microvilli. With immunofluorescence, we were able to demonstrate the presence of both filaments and round particles labeled with a monoclonal antibody to the F protein in RSV-infected HEp-2 cells. This suggests that the filaments represent viral particles budding from the cell surface microvilli, which is further supported by the presence of the N protein in the filamentous projections and microvilli.

Roberts et al. (34) demonstrated polarized maturation and budding of RSV from the host membrane, suggesting clustering of the virus prior to its release from the host cell. This selective targeting of virus has been demonstrated for other viruses and their proteins, including influenza virus and its HA protein (36, 45). Specifically, influenza virus, measles virus, Ebola virus, and HIV have been shown to incorporate into the lipid microdomains of the host cell and bud selectively from these discrete areas. In this study, we are able to show, through both traditional sucrose density gradients and immunofluorescent microscopy, the association of RSV F glycoprotein with lipid rafts and their constitutive proteins.

Lipid microdomains, or rafts, are highly liquid-ordered areas of the plasma membrane which exist in equilibrium with adjacent nonraft domains. These microdomains are enriched in cholesterol, sphingomyelin, and both glycosylphosphatidylinositol-anchored and acylated proteins. Because of these unique characteristics, lipid rafts can be distinguished from nonraft domains. Nyguen and Hildreth demonstrated selective incorporation of HIV into lipid rafts with dialkylcarbocyanine dyes (26). $DiIC_{16}(3)$ consists of a long acyl chain, which allows its incorporation into the more rigid, ordered lipid domains, compared to $DiIC_{12}(3)$, which labels the fluid nonraft membrane components (39). To demonstrate the selective incorporation of the dyes into their respective membrane compartments, we used antibodies to both caveolin-1 and CD44. These proteins have previously been isolated from lipid rafts, and similarly, we are also able to demonstrate raft distribution of caveolin-1 and CD44 through sucrose density gradients following detergent extraction. With the DiIC dyes, we showed the

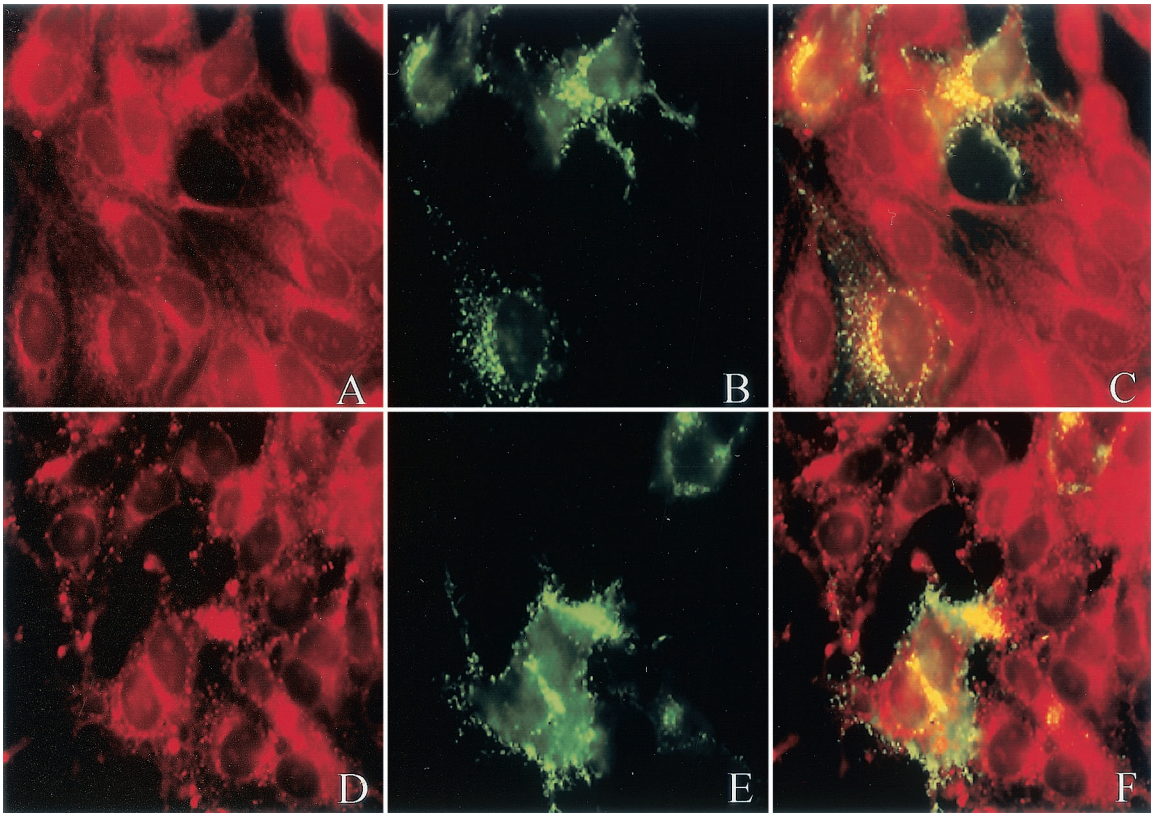

FIG. 7. Treatment of HEp-2 cells with C3 toxin prior to RSV infection blunts filament formation and alters the colocalization of F with the lipid microdomain dye. HEp-2 cells were treated with 250 μl of C3 toxin at 30 μg/ml overnight prior to infection with RSV. Cells were infected with RSV at a multiplicity of infection of 1.0 and then incubated for 24 h after RSV infection in the presence or absence of C3 toxin. Cells were then incubated with lipid dye $DiIC_{12}(3)$ (A) or $DiIC_{16}(3)$ (D) on ice (red). Cells were fixed and labeled with mouse anti-F monoclonal antibody, followed by FITC-labeled mouse anti-IgG antibody (B and E; green). Overlap between the dyes and anti-F is shown in yellow (C and F). Following treatment with C3 toxin, the viral filaments of RSV-infected cells appear shortened and relatively decreased in number. In addition, the overlap between the F protein and $DiIC_{12}(3)$, the nonraft dye, is increased, while there is diminished localization with the lipid microdomain relative to untreated cells.

overlap between the two proteins with $DiIC_{16}(3)$ and their exclusion from areas labeled with $DiIC_{12}(3)$.

Examination of images of $DiIC_{16}(3)$-stained cells demonstrated the labeling of viral filaments, while there is no evidence of filaments in $DiIC_{12}(3)$-stained cells. This suggests that RSV filaments may originate from selected areas of the membrane involving the lipid raft. Brown and colleagues recently demonstrated the presence of a lipid raft protein, caveolin-1, on the surface of budding RSV filaments by both immunofluorescent and electron microscopy (6). With monoclonal antibodies to the F protein, we were able to confirm the aggregation of F protein within the lipid rafts by showing predominant colocalization of F with the lipid microdomain dye, with nearly complete exclusion of F from the nonraft domain. While there were some areas of F staining which did not overlap with the lipid dye, and likewise few areas which overlapped with $DiIC_{12}(3)$, this finding can be explained by the highly membrane-associated nature of RSV.

Up to 90% of RSV remains cell associated, and subsequently one would anticipate overlap of RSV proteins with the nonraft domains, as the raft portion of the host membrane is the minority. This finding was also noted in Western blot analysis of RSV proteins, where viral proteins were associated with both detergent-insoluble and -soluble components of the membrane, including the envelope protein F. However, there was evidence that certain viral proteins are found predominantly in the lipid raft microdomains, including the G protein and the nucleocapsid proteins N and P. Selective targeting of F and the nucleocapsid proteins to the microdomain may initiate events that favor assembly of RSV virions in the lipid rafts. As has been suggested for HIV, coalescence of lipid raft domains at the time of virus budding may approximate viral proteins and lead to a higher density of F glycoprotein expression on infectious viral progeny. Similarly, the selective targeting of F and other RSV proteins to the cell membrane may initiate events that lead to the formation of microvillus projections and subsequent release of filamentous RSV virions from microdomains.

The interaction of actin with other cytoskeleton components is important for the formation of microvillus projections. Previous work has demonstrated a role for CD44 and the ERM (ezrin, radixin, and moesin) family of proteins in microvillus formation via actin cross-linking (22, 44). RhoA is a small GTPase which influences the formation of actin stress fibers and also leads to microvillus formation upon phosphorylation of the ERM proteins (29). In vitro, RhoA has been shown to

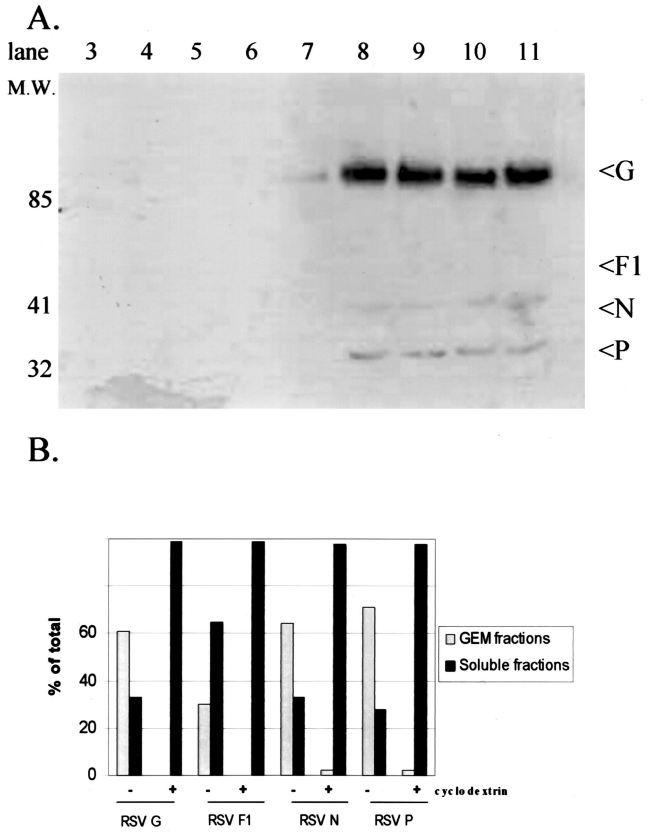

FIG. 8. Treatment of RSV-infected cells with methyl-β-cyclodextrin alters the distribution of RSV proteins within the lipid microdomains. At 24 h postinfection, RSV-infected HEp-2 cells were treated with 10 mM methyl-β-cyclodextrin for 30 min at 37°C and then lysed in 1% Triton X-100 at 4°C. Postnuclear extract was layered with a discontinuous sucrose gradient and centrifuged at 35,000 rpm for 16 h, and 1-ml fractions were collected. Fraction 1 represents the top of the gradient, and fraction 12 represents the bottom. Examination of viral proteins with a horseradish peroxidase-conjugated goat polyclonal anti-RSV antibody was performed by Western blotting after separation by sodium dodecyl sulfate-PAGE and transfer to polyvinylidene difluoride membranes (A). Quantification of viral proteins by densitometry was performed for both untreated (Fig. 3B) and cyclodextrin-treated lysates following sucrose gradient separation, and the percentage of each individual protein distributed to the lipid microdomains (fractions 3 to 6) was determined (B). RSV envelope and nucleoproteins are found within the lipid microdomain fractions. Comparison of untreated RSV-infected HEp-2 cells to cyclodextrin-treated cells demonstrates a substantial alteration in the distribution of RSV proteins following manipulation of the cholesterol content.

interact with the RSV F protein (31). In addition, RSV infection leads to both translocation of activated RhoA to the plasma membrane and a RhoA-dependent increase in stress fiber formation (11). While the in vivo relationship between RhoA and F has not been determined, we showed that RhoA is detergent insoluble at low temperature and partitions to the lipid raft portion of the sucrose gradient by Western blot analysis in RSV-infected cells.

Through immunofluorescent imaging, we confirmed colocalization of RhoA with the lipid raft dye, while showing that it is predominantly excluded from nonraft domains. With polyclonal antibody to RSV, we were also able to demonstrate an overlap of RhoA with the RSV proteins. This suggests that in RSV-infected cells, colocalization of RhoA and F occurs in membrane lipid microdomains. RhoA activation is necessary for filament formation, perhaps through direct effects on CD44 and ERM proteins. Whether a direct interaction of F with RhoA is involved in this process is not known. The possible interaction of the F protein with ERM proteins needs to be investigated further, as the rabies virus and other viruses have been described to incorporate actin-binding proteins into their virions (35).

We further demonstrated the importance of RhoA in RSV filament formation with *C. botulinum* exotoxin. C3 toxin irreversibly inactivated RhoA signaling pathways by ADP-ribosylation of RhoA. RSV-induced stress fiber formation and syncytium formation are inhibited in the presence of C3 treatment, although viral titer is unaffected (11). We showed that the morphological characteristics of RSV filaments are altered in the presence of C3 toxin. Filaments appeared blunted compared to untreated cells. Similarly, electron microscopy of C3 toxin-treated RSV-infected cells showed diminished length and number of budding filaments (Gower et al., submitted for publication). The lack of filaments may be responsible for the absence of syncytia among C3 toxin-treated cells.

In addition, the maturation site of RSV appeared to be changed by C3 toxin, as fluorescently labeled F protein is less associated with the lipid raft dye $DiIC_{16}(3)$ in the presence of C3 toxin compared to control RSV-infected cells and shows a relative increase in colocalization with $DiIC_{12}(3)$. Interference with RhoA activity may lead to abnormal targeting of viral protein to the nonraft domains of the cell surface and a subsequent lack of filaments and syncytia, thereby altering the pathogenesis of RSV. Similarly, we demonstrated that the distribution of viral proteins is significantly altered following the removal of cholesterol from the cellular membrane. Treatment of infected cells with cyclodextrin effectively disassociates RSV proteins from lipid microdomains and provides a possible new mechanism to inhibit the formation of infectious RSV virions.

RSV is an important respiratory pathogen in infants and has increasingly emerged as a cause of severe morbidity and mortality in elderly and immunocompromised hosts. The importance of the RSV F protein to the pathogenesis of syncytium formation has been well characterized, including the cytopathologic development of giant-cell pneumonia in immunocompromised hosts. We demonstrate an association of the F protein with lipid microdomains of the plasma membrane and the presence of viral filaments budding selectively from these specialized regions. As with HIV and other enveloped viruses, it suggests a preferential localization of viral proteins within the lipid microdomains, allowing favorable interactions with cellular proteins, including RhoA and CD44, that then leads to the formation of filaments, responsible for the development of syncytia. Manipulation of either the lipid component of the membrane or the incorporation of cellular or viral proteins into the microdomains may favorably alter RSV pathogenesis and provide future targets for pharmacologic therapy directed at the prevention and treatment of RSV-caused disease.

ACKNOWLEDGMENTS

This work was supported in part by National Institutes of Health grants T32 AI 07474 (Molecular Basis of Infectious Diseases Training Program) and RO1-A1-33933.

We gratefully acknowledge Manoj Pastey and Tara Gower for technical assistance.

REFERENCES

1. **Adamson, P., C. Marshall, A. Hall, and P. A. Tilbrook.** 1992. Post-translational modification of p21 Rho proteins. J. Biol. Chem. **272:**20033–20038.
2. **Bachi, T.** 1988. Direct observation of the budding and fusion of an enveloped virus by video microscopy of viable cells. J. Cell Biol. **107:**1689–1695.
3. **Bavari, S., C. M. Bosio, E. Wiegand, G. Ruthel, A. B. Will, T. W. Geisbert, M. Hevey, C. Schmaljohn, A. Schmaljohn, and M. J. Aman.** 2002. Lipid raft microdomains: a gateway for compartmentalized trafficking of Ebola and Marburg viruses. J. Exp. Med. **195:**593–602.
4. **Brown, D. A., and E. London.** 1998. Functions of lipid rafts in biological membranes. Annu. Rev. Cell Dev. Biol. **14:**111–136.
5. **Brown, D. A., and J. K. Rose.** 1992. Sorting of glycosylphosphatidylinositol-anchored proteins to glycolipid-enriched membrane subdomains during transport to the apical cell surface. Cell **68:**533–544.
6. **Brown, G., J. Aitken, H. W. McL. Rixon, and R. J. Sugrue.** 2002. Caveolin-1 is incorporated into mature respiratory syncytial virus particles during virus assembly on the surface of virus-infected cells. J. Gen. Virol. **83:**611–621.
7. **Brown, G., H. W. M. Rixon, and R. J. Sugrue.** 2002. Respiratory syncytial virus assembly occurs in GM1-rich regions of the host-cell membrane and alters the cellular distribution of tyrosine phosphorylated caveolin-1. J. Gen. Virol. **83:**1841–1850.
8. **Falsey, A. R., E. E. Walsh, and R. F. Betts.** 1990. Serologic evidence of respiratory syncytial virus in nursing home patients. J. Infect. Dis. **162:**569–570.
9. **Faulkner, G., P. V. Shirodaria, E. A. C. Follett, and C. R. Pringle.** 1976. Respiratory syncytial virus temperature-sensitive mutants and nuclear immunofluorescence. J. Virol. **20:**487–500.
10. **Feldman, S. A., R. M. Hendry, and J. A. Beeler.** 1999. Identification of a linear heparin binding domain for human respiratory syncytial virus attachment glycoprotein G. J. Virol. **73:**6610–6617.
11. **Gower, T., M. E. Peebles, P. L. Collins, and B. S. Graham.** 2001. RhoA is activated during respiratory syncytial virus infection. Virology **283:**188–196.
12. **Gower, T. L., and B. S. Graham.** 2001. Antiviral activity of lovastatin against respiratory syncytial virus in vivo and in vitro. Antimicrob. Agents Chemother. **45:**1231–1237.
13. **Graham, B. S., M. D. Perkins, P. F. Wright, and D. T. Karzon.** 1988. Primary respiratory syncytial virus infection in mice. J. Med. Virol. **26:**153–162.
14. **Hall, A.** 1998. Rho GTPases and the actin cytoskeleton. Science **279:**509–514.
15. **Han, L. L., J. P. Alexander, and L. J. Anderson.** 1999. Respiratory syncytial virus pneumonia among the elderly: an assessment of disease burden. J. Infect. Dis. **179:**25–30.
16. **Harrington, R. D., T. M. Hooton, R. C. Hackman, G. A. Storch, B. Osborne, C. A. Gleaves, A. Benson, and J. D. Meyers.** 1992. An outbreak of respiratory syncytial virus in a bone marrow transplant center. J. Infect. Dis. **165**:987–993.
17. **Kahn, J. S., M. J. Schnell, L. Buonocore, and J. K. Rose.** 1999. Recombinant vesicular stomatitis virus expressing respiratory syncytial virus (RSV) glycoproteins: RSV fusion protein can mediate infection and cell fusion. Virology **254:**81–91.
18. **Kjoller, L., and A. Hall.** 1999. Signaling to Rho GTPases. Exp. Cell Res. **253:**166–179.
19. **Krusat, T., and H. J. Streckert.** 1997. Heparin-dependant attachment of respiratory syncytial virus (RSV) to host cells. Arch. Virol. **142:**1247–1254.
20. **Levine, S., R. Klaiber-Franco, and P. R. Paradiso.** 1987. Demonstration that glycoprotein G is the attachment protein of respiratory syncytial virus. J. Gen. Virol. **68:**2521–2524.
21. **Liao, Z., L. M. Cimakasky, R. Hampton, D. H. Nguyen, and J. E. K. Hildreth.** 2001. Lipid rafts and HIV pathogenesis: Host membrane cholesterol is required for infection by HIV type 1. AIDS Res. Hum. Retrovir. **27:**1009–1019.
22. **Louvet-Vallee, S.** 2000. ERM proteins: from cellular architecture to cell signaling. Biol. Cell **92:**305–316.
23. **Manes, S., G. del Real, R. A. Lacalle, P. Luca, C. Gomez-Mouton, S. Sanchez-Palomino, R. Delgado, J. Alcami, E. Mira, and C. Martinez-A.** 2000. Membrane raft microdomains mediate lateral assemblies required for HIV-1 infection. EMBO Rep. **1:**190–196.
24. **Manie, S. N., S. Debreyne, S. Vincent, and D. Gerlier.** 2000. Measles virus structural components are enriched into lipid raft microdomains: a potential cellular location for virus assembly. J. Virol. **74:**305–311.
25. **Narumiyz, S.** 1996. The small GTPase Rho: cellular functions and signal transduction. J. Biochem. **120:**215–228.
26. **Nguyen, D. H., and J. E. K. Hildreth.** 2000. Evidence for budding of human immunodeficiency virus type 1 selectively from glycolipid-enriched membrane lipid rafts. J. Virol. **74:**3264–3272.
27. **Oliferenko, S., K. Paiha, T. Harder, V. Gerke, C. Schwarzler, H. Schwarz, H. Beug, U. Gunthert, and L. A. Huber.** 1999. Analysis of CD44-containing lipid rafts: recruitment of annexin II and stabilization by the actin cytoskeleton. J. Cell Biol. **146:**843–854.
28. **Ono, A., and E. O. Freed.** 2001. Plasma membrane rafts play a critical role in HIV-1 assembly and release. Proc. Natl. Acad. Sci. USA **98:**13925–13930.
29. **Oshiro, N., Y. Fukata, and K. Kaibuchi.** 1998. Phosphorylation of moesin by Rho associated kinase (Rho-kinase) plays a crucial role in the formation of microvillus-like structures. J. Biol. Chem. **273:**34663–34666.
30. **Palmer, S. M., N. G. Henshaw, D. N. Howell, S. E. Miller, R. D. Davis, and V. F. Tapson.** 1998. Community respiratory viral infection in adult lung transplant recipients. Chest **113:**944–950.
31. **Pastey, M. K., J. E. Crowe, Jr., and B. S. Graham.** 1999. RhoA interacts with the fusion glycoprotein of respiratory syncytial virus and facilitates virus-induced syncytium formation. J. Virol. **73:**7262–7270.
32. **Pastey, M. K., T. L. Gower, P. Spearman, J. E. Crowe, and B. S. Graham.** 2000. A RhoA derived peptide inhibits syncytium formation induced by respiratory syncytial virus and parainfluenza virus type 3. Nat. Med. **6:**35–40.
33. **Ridley, A. J., and A. Hall.** 1992. The small GTP binding protein Rho regulates the assembly of focal adhesions and actin stress fibers in response to growth factors. Cell **70:**389–399.
34. **Roberts, S. R., R. W. Compans, and G. W. Wertz.** 1995. Respiratory syncytial virus matures at the apical surfaces of polarized epithelial cells. J. Virol. **69:**2667–2673.
35. **Sagara, J., S. Tsukita, S. Yonemura, S. Tsukita, and A. Kawai.** 1995. Cellular actin binding ezrin-radixin-moesin (ERM) family proteins are incorporated into the rabies virion and closely associated with viral envelope proteins in the cell. Virology **206:**485–494.
36. **Scheiffele, P., A. Rietveld, T. Wilk, and K. Simons.** 1999. Influenza viruses select ordered lipid domains during budding from the plasma membrane. J. Biol. Chem. **274:**2038–2044.
37. **Shay, D. K., R. C. Holman, R. D. Newman, L. L. Liu, J. W. Stout, and L. J. Anderson.** 1999. Bronchiolitis-associated hospitalizations among US children, 1980–1996. JAMA **282:**1440–1446.
38. **Simons, K., and E. Ikonen.** 1997. Functional rafts in cell membranes. Nature **385:**569–572.
39. **Spink, C. H., M. D. Yeager, and G. W. Feigenson.** 1990. Partitioning behavior of indocarbocyanine probes between coexisting gel and fluid phases in model membranes. Biochim. Biophys. Acta **1023:**25–33.
40. **Techaarpornkul, S., N. Barretto, and M. E. Peebles.** 2001. Functional analysis of recombinant respiratory syncytial virus deletion mutants lacking the small hydrophobic and/or attachment glycoprotein gene. J. Virol. **75:**6825–6834.
41. **Walsh, E. E., and J. Hruska.** 1983. Monoclonal antibodies to respiratory syncytial virus proteins: identification of the fusion protein. J. Virol. **47:**171–177.
42. **Wendt, C. H., J. M. K. Fox, and M. I. Hertz.** 1995. Paramyxovirus infection in lung transplant recipients. J. Heart Lung Transplant. **14:**479–485.
43. **Wessel, D., and U. I. Flugge.** 1984. A method for the quantitative recovery of protein in dilute solution in the presence of detergents and lipids. Anal. Biochem. **138:**141–143.
44. **Yonemura, S., M. Hirao, Y. Doi, N. Takahashi, T. Kondo, S. Tsukita, and S. Tsukiata.** 1998. Exrin/radixin/moesin (ERM) proteins bind to a positively charged amino acid cluster in the juxta-membrane cytoplasmic domain of CD44, CD43, and ICAM-2. J. Cell Biol. **140:**885–895.
45. **Zhang, J., A. Pekosz, and R. A. Lamb.** 2000. Influenza virus assembly and lipid raft microdomains: a role for the cytoplasmic tails of the spike glycoproteins. J. Virol. **74:**4634–4644.